

# Development of a personal dosimeter badge system using sintered LiF:Mg,Cu,Na,Si TL detectors for photon fields

Haiyong Jung<sup>a,\*</sup>, Kun Jai Lee<sup>a</sup>, Jang-Lyul Kim<sup>b</sup>, Sang-Yoon Lee<sup>b</sup>

<sup>a</sup>Department of Nuclear and Quantum Engineering, Korea Advanced Institute of Science and Technology (KAIST), 373-1 Guseong-dong, Yuseong-gu, Daejeon 305-701, South Korea

<sup>b</sup>Korea Atomic Energy Research Institute (KAERI), P.O. Box 105, Yuseong, Daejeon 305-600, South Korea

Received 26 November 2002; received in revised form 15 August 2003; accepted 17 August 2003

## Abstract

The badge system of personal thermoluminescence (TL) dosimeter for photon fields using LiF:Mg,Cu,Na,Si TL material, which was developed by Korea Atomic Energy Research Institute (KAERI) a few years ago, was developed by taking advantage of its dosimetric properties including energy dependencies. A badge filter system was designed by practical irradiation experiments supported by computational modeling using Monte Carlo simulation. Design properties and dosimetric characteristics such as photon energy response and angular dependence of new TL dosimeter system examined through the irradiation experiments are presented. Based on the experiments for the developed dosimeter, it is demonstrated that the deep dose response of dosimeter provided the value between 0.78 and 1.08, which is within the design limit by ISO standard. This multi-element TL dosimeter badge system allows the discrimination of the incident radiation type between photon and beta by using the ratios of the four TL detectors. Personal TL dosimeter using sintered LiF:Mg,Cu,Na,Si TL detectors has the ability to measure a personal dose equivalent  $H_p(d)$  for a wide range of photon energies.

© 2003 Elsevier Ltd. All rights reserved.

**Keywords:** LiF:Mg,Cu,Na,Si; Thermoluminescence; Personal dosimeter; Filter system

## 1. Introduction

Thermoluminescence dosimetry is the most widely used technology for evaluating the personal and environmental radiation exposure. Lithium fluoride (LiF) is a well-known thermoluminescent (TL) dosimetry material used in environmental and personal monitoring due to its high sensitivity, stability and tissue-equivalency.

The first interest in the thermoluminescent phenomenon of LiF for dosimetry was by Daniel et al. (1953) from the University of Wisconsin. Since then many experimental doping agents were used with LiF. The TLD material based on LiF that has been studied most extensively is LiF:Mg,Ti, which is widely used in personal dosimetry and available in the

market under trade names like TLD-100 and its variations, TLD-600 and TLD-700 which contain different concentrations of lithium isotopes (Vij, 1993). Since the introduction of LiF:Mg,Ti (TLD-100), many new types of TL materials have been developed and used to evaluate the personal dose equivalent in various radiation fields. Many researches for developing the more advanced thermoluminescence materials have been accomplished. Nakajima et al. (1978) were the first to describe the properties of LiF doped with Mg, Cu and P impurities, namely, a high sensitivity and a good tissue equivalency. This material, LiF:Mg,Cu,P, has been improved and commercialized by Chinese (GR-200), Polish (MCP-N) and USA (TLD-100H, TLD-600H, TLD-700H) (Bos, 2001).

In Korea, Doh et al. (1989) developed powdered type of LiF doped with magnesium, copper, sodium and silicon, and undertook a study on its characteristics about a wide range of dopants concentration in the 1980s. After Doh et al. proposed LiF doped with four dopants, Kim et al. (1989)

\* Corresponding author. Tel.: +82-42-869-3858; fax: +82-42-869-3810.

E-mail address: [hyjung@nuchen.kaist.ac.kr](mailto:hyjung@nuchen.kaist.ac.kr) (H. Jung).

found out that the response of LiF:Mg,Cu,Na,Si for low energy photons was higher than that of LiF:Mg,Cu,P in the aspect of dosimetric property. In the 1990s, more concrete researches on the powder type LiF:Mg,Cu,Na,Si TL phosphor have been accomplished by Korea Atomic Energy Research Institute (KAERI) (Nam et al., 1998, 1999). This powder type TL phosphor has about 2 times higher sensitivity in comparison with LiF:Mg,Cu,P. However, the powder type TL phosphor has many disadvantages for the practical handling of the material. Therefore, it is necessary to develop a suitably shaped solid type TL detector for application in practical dosimetry fields. During the last few years the LiF:Mg,Cu,Na,Si TL material has been studied for practical pellet type TL detector by Nam Y.M. et al., the dosimetry group of health physics department in KAERI (Nam et al., 2000). But the sensitivity of developed pellet type TL detectors did not exceed 50% of Chinese GR-200A, and had poor reusability, that is, a decrease of 10% of the readout values after a reuse of 8 times (Nam et al., 2001). Based on these previous studies by Nam et al., the sensitivity and reusability of the pellet type LiF:Mg,Cu,Na,Si TL detectors were improved by modification of the dopants concentration and the parameters of the preparing procedure. The optimum concentration of dopants for pellet type LiF:Mg,Cu,Na,Si TL detectors was investigated as Mg: 0.2 mol%, Cu: 0.05 mol%, Na: 0.9 mol% and Si: 0.9 mol% (Lee et al., 2002). Now a days, it has become possible to produce a mechanically stable and efficient TL detector using LiF:Mg,Cu,Na,Si, which is a newly developed TL material in a personal TL dosimetry field.

The objective of this study was to design and develop the badge system of a multi-element personal TL dosimeter using LiF:Mg,Cu,Na,Si TL detectors by taking advantage of its sensitivity, tissue-equivalency and energy dependencies to allow the measurement of personal dose equivalent  $H_p(d)$ . The design of dosimeter was accomplished by the practical irradiation experiments that are supported by a computational simulation with MCNP code, and then the developed dosimeter was tested in terms of its dosimetric characteristics such as photon energy response and angular dependence.

## 2. Sintered LiF:Mg,Cu,Na,Si TL detector

The TL detectors used in this study are sintered pellets made of LiF:Mg,Cu,Na,Si powder prepared by the KAERI. The detector is in the shape of a disk having a diameter of 4.5 mm and a thickness of 0.8 mm and white in color. It was made from LiF:Mg,Cu,Na,Si powder with concentration of dopants: Mg: 0.2 mol%, Cu: 0.05 mol%, Na: 0.9 mol% and Si: 0.9 mol% through cold pressing and sintering the powder at 825°C (Lee et al., 2002).

The typical glow-curve of this TL detector and of the Chinese GR-200A (LiF:Mg,Cu,P) presented in Fig. 1 show that the TL intensity of LiF:Mg,Cu,Na,Si is about 15%

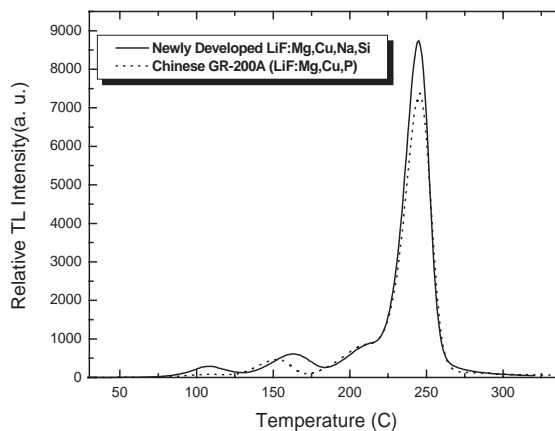


Fig. 1. Glow-curve and comparison TL intensity of LiF:Mg,Cu,Na,Si detector and Chinese GR-200A (LiF:Mg,Cu,P). The TL detectors were irradiated to 10 mGy with  $^{137}\text{Cs}$   $\gamma$ -rays at KAERI. The measurements were carried out with a linear heating rate of 10°C/s using a commercial TLD reader (System 310, Teledyne Brown Engineering).

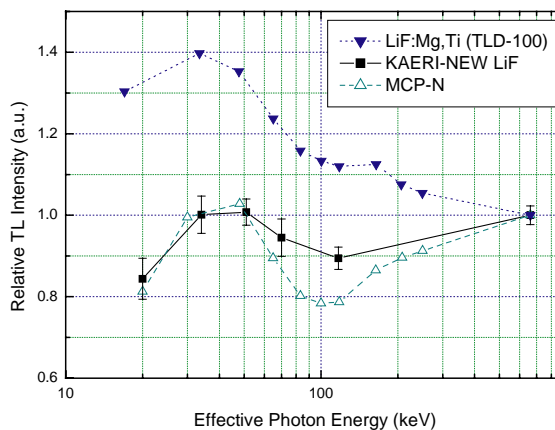


Fig. 2. Energy response of LiF:Mg,Cu,Na,Si TL detector, LiF:Mg,Ti (TLD-100) and LiF:Mg,Cu,P (MCP-N, Poland) free in air. Responses are normalized to 662 keV photons from a  $^{137}\text{Cs}$  source.

higher than that of GR-200A which is widely used in the world. The energy dependence of new LiF:Mg,Cu,Na,Si detector and of other common TL materials are shown in Fig. 2. The energy dependence of TL material, as described previously, is a key factor and plays an important role in designing the TL dosimeter filter system. Relative photon energy response of TL detector was measured in the free air conditions. Six TL detectors were placed at 200 cm away from the radiation source (five X-ray beams and the  $^{137}\text{Cs}$ ), mounted on a polyethylmethacrylate plate with a density of 1.19 g/cm<sup>3</sup> with a front face area of 10 cm × 10 cm and a thickness of 2 mm. TL detectors were covered with a polyethylene film (with a density thickness of 1.9 mg/cm<sup>2</sup>) for five X-ray beams and with a polyethylmethacrylate

plate with a thickness of 2 mm for  $^{137}\text{Cs}$  to consider the electron equilibrium. The measured relative response to 662 keV photons of  $^{137}\text{Cs}$  for LiF:Mg,Cu,Na,Si TL detector and other common TL detectors in bare condition are presented as a function of the mean photon energies. The energy dependence of LiF:Mg,Ti (TLD-100) detector and that of LiF:Mg,Cu,P (MCP-N) detectors are presented together to compare the results of LiF:Mg,Cu,Na,Si TL detector. The data of LiF:Mg,Cu,P (MCP-N) detectors are contained in the research by Budzanowski et al. (2001). The research by Budzanowski et al. (2001) presented the energy response of LiF:Mg,Cu,Na,Si detector and that of LiF:Mg,Cu,P (MCP-N). LiF:Mg,Cu,Na,Si detector in the research by Budzanowski et al. differs from the detector by Lee et al. (2002) who modified and set the optimum dopants concentration and the parameters of preparing procedure to improve the sensitivity and reusability of the detector. Therefore, the energy dependence of LiF:Mg,Cu,Na,Si detector in this study differs from the result of Budzanowski. While the energy response of LiF:Mg,Ti is different from two others, the energy response between LiF:Mg,Cu,P and LiF:Mg,Cu,Na,Si has a similar curve. However, the LiF:Mg,Cu,Na,Si TL detector shows that it can reduce the variation of response between 30 and 662 keV, compared with MCP-N. The energy response curve of LiF:Mg,Cu,Na,Si detector is almost flat and this is a good characteristic for designing the dosimeter.

### 3. Computational modeling with Monte Carlo simulation

The data for the dosimetric properties and energy dependence of TL material are essential to develop the TL badge system, but it is difficult to get enough data because of time-consuming and limited experiments. Computational modeling with Monte Carlo simulation is suitable for solving the problem resulting from limited experiments through pre-estimation of energy dependence of TL material in various conditions. In general, it is finally based on the irradiation experiments to choose filter

material and to determine the geometric figures of dosimeter by considering the information on the current practical TL dosimeter and the requirement to measure the personal dose equivalent. The main objective of computational modeling is to pre-estimate the energy response of TL detector in various environments and to verify the results from experiments.

In this study, Monte Carlo particle transport code, MCNP-4C (RSICC, 2000) developed by the Los Alamos National Laboratory, which is the representative irradiation transport code used for the general purpose of Monte Carlo simulation, is used. First of all, it is necessary to calibrate the MCNP code estimation of bare TL detector without any filters against the experimental readout of the bare TL detectors for the photon fields. The calibrated MCNP results are then used in subsequent MCNP calculations to pre-estimate and verify the energy response of the dosimeter.

The irradiation geometry of the TL detector and the experimental conditions in the Monte Carlo simulation are set to be same as the real experiment as shown in Fig. 3. The badge system was modeled at 200 cm away from the radiation source, mounted at the center of a tissue equivalent phantom, facing towards the source. The phantom was assumed as a homogeneous PMMA (polyethylmethacrylate) slab with a density of  $1.19 \text{ g/cm}^3$  with a front face area of  $30 \text{ cm} \times 30 \text{ cm}$  and a thickness of 15 cm. The air medium between the radiation source and the phantom was included in the MCNP calculations.

The radiation source was modeled as a point mono-directional irradiation field of the X-ray (M30, M60, M100, M150, H150) of KAERI and the  $^{137}\text{Cs}$  radiation fields with a disc radius 15 cm such that it covers the sides of the phantom. Photons leaving the source were incident normally on the badge and the phantom. The mono-directional beam source was chosen due to the small solid angle between the source and the badge, and due to the large source to phantom distance compared with the dimensions of the badge. Fig. 3 represents a geometrical configuration of the model plotted with SABRINA used in the simulation (ORNL, 1994). This model was fixed for all subsequent MCNP

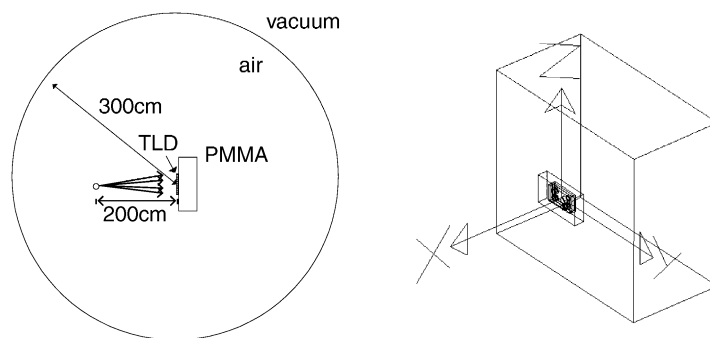


Fig. 3. Geometrical configuration of MCNP modeling of TLD response calculation.



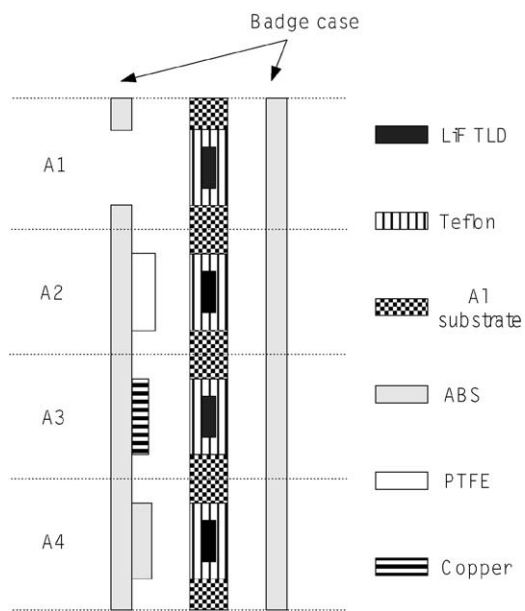


Fig. 4. Schematic cross section of the proposed TL dosimeter.

of Teflon, 0.05 mm ( $11 \text{ mg/cm}^2$ ) thick and mounted on an aluminum substrate. All of the detectors are fabricated from newly developed  $\text{LiF:Mg,Cu,Na,Si}$  material. The badge case is made of 1.0 mm thick ABS (Polyacrylonitrile–Butadiene–Styrene) plastic material which is the most reliable and stable plastic among many plastic materials under the condition of radiation field. The effect of the plastic badge case was also considered in the analysis of the filter design in each

Table 2  
Characteristics of the filter system for the proposed TL dosimeter

Area	Filter material	Density ( $\text{g/cm}^3$ )	Thickness of filter (mm)	Total density thickness ( $\text{mg/cm}^2$ )
A1	Teflon (card)	2.2	0.05	11
A2	Teflon (card)	2.2	0.05	995
	ABS Plastic	1.04	1.0	
A3	PTFE	2.2	4.0	563
	Teflon (card)	2.2	0.05	
	ABS Plastic	1.04	1.0	
A4	Copper	8.96	0.5	323
	Teflon (card)	2.2	0.05	
	ABS Plastic	1.04	3.0	

area of the badge. Each detector/filter combination performs a specific function, as follows: For open window area, a TL detector with 0.05 mm Teflon encapsulation determines the shallow dose. The filtration for this element is  $11 \text{ mg/cm}^2$ . No additional filter material is needed to measure the shallow dose in the A1 area since the density thickness of Teflon encapsulation of TL detector is  $11 \text{ mg/cm}^2$ . Another TLD with  $995 \text{ mg/cm}^2$  combined PTFE/ABS filtration ( $104 \text{ mg/cm}^2$  ABS +  $880 \text{ mg/cm}^2$  PTFE filters) measures the deep dose in the A2 area. The third TLD covered with  $104 \text{ mg/cm}^2$  ABS plastic and  $448 \text{ mg/cm}^2$  copper filtration is used for low energy photon discrimination. The last TLD is covered with  $323 \text{ mg/cm}^2$  ABS plastic for energy discrimination for beta particles.



Fig. 5. Photograph of  $\text{LiF:Mg,Cu,Na,Si}$  detectors and the newly developed dosimeter.

*Open window area (A1)*: This area is required to have a capacity for indicating the dose delivered at depth of 0.07 mm under the tissue,  $H_p(0.07)$ . The TL detector is covered with Teflon film at a density thickness of 11 mg/cm<sup>2</sup> as a card encapsulation. Since this Teflon encapsulation meets the required density thickness, no additional filter material is needed to measure the shallow dose at the depth of 0.07 mm. With this arrangement, the TL detector in the open window area responds to both beta and photon.

*Deep dose area (A2)*: This area is designed to measure the deep dose with an appropriate filter. The response of the TL material under this filter will indicate the deep dose equivalent delivered to tissue at a depth of 1.0 cm. Since LiF is a tissue equivalent material close to the tissue composition, it would not be necessary to design additional filter. Only the plastic filter for measuring radiation dose to tissue at a depth of 1.0 cm is necessary. Poly-tetrafluoro-ethylene (PTFE) plastic filter whose thickness is about 4 mm could be used to meet this objective measuring the deep dose, i.e., to have 1000 mg/cm<sup>2</sup> density thickness. In addition to the objective of measuring the deep dose of this area, this area will play a part in shielding the beta radiation. For beta shield, this area should be designed to attenuate at least 97% of Sr<sup>90</sup>/Y<sup>90</sup> beta radiation, such that when the response of this area is compared with the open window response, the proper contribution of this beta radiation to the shallow dose can be measured. The above goals are required to allow for proper discrimination of response in the case of mixed beta/gamma exposure. Since the purpose of this is to shield only against beta radiation, it should provide little attenuation of gamma radiation.

*Energy discrimination area (A3 & A4)*: The badge system should be able to resolve the readout in case of exposure to mono-energetic photons or to a mixture of high- and low-energy photons or a mixture of photons and beta ray. This may be achieved by utilizing ratios of readout. A3 and A4 region is necessary for making the combination of response ratio of each area since they have different response from that of A1 or A2. For the case of a mono-energetic

gamma ray exposure, or a single X-ray effective energy, the ratio of the deep dose area readout to that of this area, (A1/A3), may be used to indicate the effective energy of the radiation source. From 20 keV on, this ratio decreases as the effective energy increases. It seems that the response of A4 area does not differ from that of A1 area since the filter material is relatively thin plastic. This area is, however, for supporting the discrimination of radiation type between photon and beta particles by making the combination of response ratio.

## 5. Irradiation experiments

The LiF:Mg,Cu,Na,Si TL detector described in the previous section was used for dosimeter badge system in irradiation experiments. The irradiation experiments of the proposed TL dosimeter badge system for energy response experiments were carried out at the KAERI using <sup>137</sup>Cs and X-ray beam (ANSI X-ray beam code M30, M60, M100, M150, H150) produced to meet the Korea national X-ray test standard (Kim et al., 1997). Specifications for each X-ray technique used in this experiment are given in Table 3. For the angular dependence test, the factors to convert from air kerma to deep dose equivalent for irradiations at non-perpendicular incidence and angular response factors (ARF) for the deep dose equivalent for X-ray beam are listed in Table 4 (ANSI, 1999). The reference X-ray fields constructed in the KAERI consists of two types of X-ray machines, the low-energy system and the medium system. Low-energy X-ray system is 3.0 kW grade (Pantak, HF-75c) and a beryllium plate of 1.0 mm is installed as inherent filters. Medium-energy X-ray system is 3.2 kW grade (Phillips, MG325) and the inherent filter consists of Be (4 mm) + Al (1.5 mm). After the irradiation experiment, the TELEDYNE TLD Reader System 310 with ohmic heating systems is used for readout. All gamma photon readouts are given relative to <sup>137</sup>Cs and related correction factors were used to minimize statistical fluctuations in the system (Moscovitch, 1993).

Table 3  
Properties of reference X-ray technique used for energy response simulation and experiments at KAERI<sup>a</sup>

X-ray beam	$E_{\text{eff}}$ (keV)	H.V. (kVp)	Current (mA)	$K_a$ (mGy/h)	Conversion coefficient <sup>b</sup> (Sv/Gy)	
					$H_p(10)/K_a$	$H_p(0.07)/K_a$
ANSI M30	19.4	30	3	255.1	0.42	1.02
ANSI M60	35.2	60	3	199.1	1.00	1.21
ANSI M100	51.2	100	3	195.5	1.52	1.49
ANSI M150	73.0	150	3	232.5	1.78	1.64
ANSI H150	118.3	150	20	31.8	1.71	1.60

<sup>a</sup>This is from the research of Kim (Kim et al., 1997).

<sup>b</sup>This is from ANSI N13.11 (ANSI, 1999).

Table 4

Factors to convert from air kerma to deep dose equivalent for irradiations at non-perpendicular incidence and angular response factors (ARF) for the deep dose equivalent for X-ray beam

Beam code	Deep dose equivalent conversion factor [Sv/Gy] <sup>a</sup>			Angular response factor (ARF) <sup>b</sup> for deep dose equivalent	
	$\alpha = 0^\circ$	$\alpha = 40^\circ$	$\alpha = 60^\circ$	$\alpha = 40^\circ$	$\alpha = 60^\circ$
ANSI M30	0.42	0.34	0.22	0.81	0.52
ANSI M60	1.00	0.89	0.68	0.89	0.68
ANSI M100	1.52	1.39	1.14	0.91	0.75
ANSI M150	1.78	1.65	1.40	0.93	0.79
ANSI H150	1.71	1.61	1.40	0.94	0.82
<sup>137</sup> Cs	1.21	1.20	1.16	0.99	0.96

<sup>a</sup>This is from ANSI N13.11 (ANSI, 1999).

<sup>b</sup>Note that  $ARF = H_p(10, \alpha) / H_p(10, 0^\circ)$ . This was obtained from deep dose equivalent conversion factor in left side.

## 6. Results and discussion

### 6.1. Energy response of the proposed dosimeter badge system

As mentioned in the previous section, the dosimeter badge system designed in this study has four main regions for photon radiation dosimetry. Each of these areas contains a typical set of filters to estimate a personal dose equivalent  $H_p(d)$  and dosimetric information. The energy response of the proposed TL dosimeter badge system was accomplished to verify the computational response of each area and to obtain more information such as response ratio.

The deep dose area (A2) was designed to measure the photon dose at a tissue depth of 10 mm,  $H_p(10)$ . As mentioned in advance, PTFE plastic filter with its about 4 mm thickness was utilized based on the experiment results and the consideration about other requirements of filter systems. To meet the purpose of this area, the filters used should be able to cut off beta radiation. The calculated and experimental energy response results of dosimeter in the deep dose area are shown in Fig. 6. As shown in Fig. 6, A2 area appears to provide relative response values in the range between 0.78 and 1.08 over the photon energy range from 20 to 662 keV. This is within the  $\pm 30\%$  design limits required by the ISO standard (ISO, 1984). Given the responses in terms of absorbed dose with  $H_p(10)$  are proportional to the dosimeter reading, therefore, without application of any sophisticated algorithm this design would enable us to simply determine the deep dose equivalent. In Fig. 7, the energy response of three areas to dose equivalent  $H_p(10)$  is presented. The energy responses of each area show their characteristics with different filter materials.

To verify the effectiveness of area A3, typical results of response ratios are illustrated in Fig. 8 as a function of effective photon energy. As shown in Fig. 8, the ratio A1/A3, where A3 represents the readout under the discrimination filter, could present the effective photon energy since the ratio A1/A3 decreases as the effective photon energy increases.

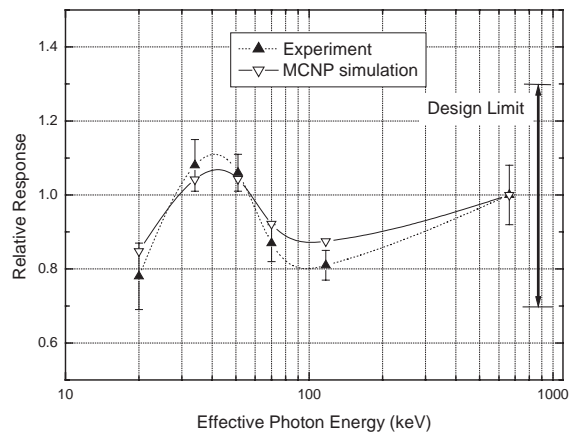


Fig. 6. The energy response of the deep dose area (A2) with personal dose equivalent,  $H_p(10)$ . Results are relative to <sup>137</sup>Cs.

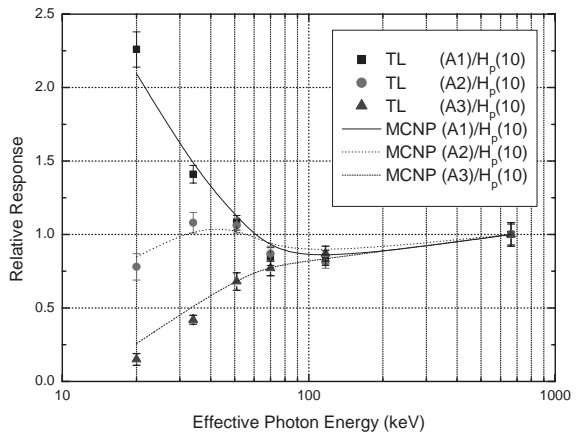


Fig. 7. Energy response of each area with respect to dose equivalent,  $H_p(10)$  obtained by MCNP and experiment. Results are relative to <sup>137</sup>Cs.

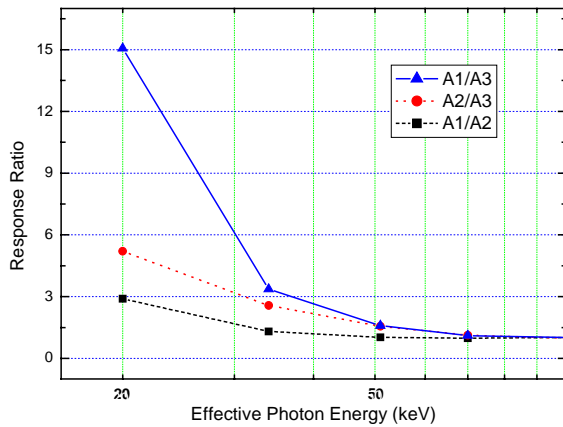


Fig. 8. Response ratio of each element.

The energy discrimination filter area in the proposed badge system was designed using a 0.5 mm copper filter as described in the previous section. For example, if the ratio A1/A3 is 6, it could be identified that the effective photon energy is about 30 keV in Fig. 8.

In addition, A4 area plays a role in discriminating the energy in the mixed field of the low-energy photon and beta particle. The irradiation test of dosimeter in the beta field of  $^{90}\text{Sr}/^{90}\text{Y}$  was achieved to check the ability to discriminate photon and beta field. The dosimeter mounted on PMMA slab phantom with a front face area of  $30\text{ cm} \times 30\text{ cm}$  and a thickness of 5 cm was placed at 35 cm away from  $^{90}\text{Sr}/^{90}\text{Y}$  source, which is the standard PTB (Physikalisch Technische Bundesanstalt) source and has a beam flattening filter, at KAERI. The dosimeter was irradiated to 10 mSv in the beta field of  $^{90}\text{Sr}/^{90}\text{Y}$ . Table 5 shows the difference of response of dosimeter between photon field and beta field of  $^{90}\text{Sr}/^{90}\text{Y}$  and the ratio of each dosimeter area. Responses are relative to  $^{137}\text{Cs}$ . The value of A1/A3 in the case of being exposed in the beta field of  $^{90}\text{Sr}/^{90}\text{Y}$  is larger than in the case of the photon field enough to discriminate the incident radiation type between X-ray beam and beta source. Moreover, the value of  $(A1 \times A4)/(A2 \times A2)$  in the beta

fields of  $^{90}\text{Sr}/^{90}\text{Y}$  is about 190, while the value in the photon field does not exceed about 7. Therefore, it is expected that these ratios make the discrimination between photon or X-ray and beta fields clear and efficient because these ratios present a distinguishing number in case of being exposed in the beta fields than in photon fields. These ratios mentioned in this part are simple examples for the discrimination of incident radiation type and there might be many other ratios which come from the combination of the four TL detectors. Therefore, more elaborate works like the selection of appropriate ratio of energy response for energy discrimination in case of mixed radiation fields are required to show the ability to discriminate the incident radiation type and determine the mixture fractions in mixed radiation fields. Dose assessment algorithm based on these works is essential to the performance test of developed TL dosimeter. Dose assessment algorithm of the proposed TL dosimeter and performance test will be accomplished in further study.

## 6.2. Angular dependence

The angular dependence test of the developed dosimeter was carried out as shown in Fig. 9. The angular dependence of the deep dose area (A2) of the dosimeter in terms of TL output per the 8.76 mGy air kerma is presented in Fig. 10. This test was performed for  $0^\circ$ ,  $20^\circ$ ,  $40^\circ$ ,  $60^\circ$ ,  $85^\circ$  angle of incidence and for two X-ray beams with an effective energy of 35.2, 118.3 and 662 keV photon from  $^{137}\text{Cs}$ . The responses are normalized to normal incidence ( $0^\circ$ ).

As can be seen in Fig. 10, for  $^{137}\text{Cs}$  a slight decrease in angular response was seen within the  $40^\circ$ , but the response after  $60^\circ$  decreased rapidly and reached around 0.78 at  $85^\circ$ . As expected, the high energy photon of  $^{137}\text{Cs}$  has less angular dependence than the low-energy photon such as X-ray beam M60. To understand more about the angular dependence of dosimeter, the results in angular dependence in Fig. 10 are supposed to be compared with the angular response factors (ARF) in Table 4. The comparison between the measured angular response of dosimeter and ARF is listed in Table 6. The angular dependence of the dosimeter seems to be similar with the ARF based on the

Table 5  
Energy response and ratios of each area for discrimination between beta and photon

Beam	$E_{\text{eff}}$ (keV)	Relative response				Response ratio	
		A1	A2	A3	A4	A1/A3	$(A1 \times A4)/(A2 \times A2)$
ANSI M30	19.4	2.26	0.78	0.15	1.73	15.07	6.43
ANSI M60	35.2	1.41	1.08	0.42	1.30	3.36	1.57
ANSI M150	73.0	0.85	0.87	0.77	0.84	1.10	0.94
$^{137}\text{Cs}$	662	1.00	1.00	1.00	1.00	1.10	1.00
$^{90}\text{Sr}/^{90}\text{Y}$	2284	1.08	0.05	0.03	0.44	36.0	190.1

Response results are relative to  $^{137}\text{Cs}$ .

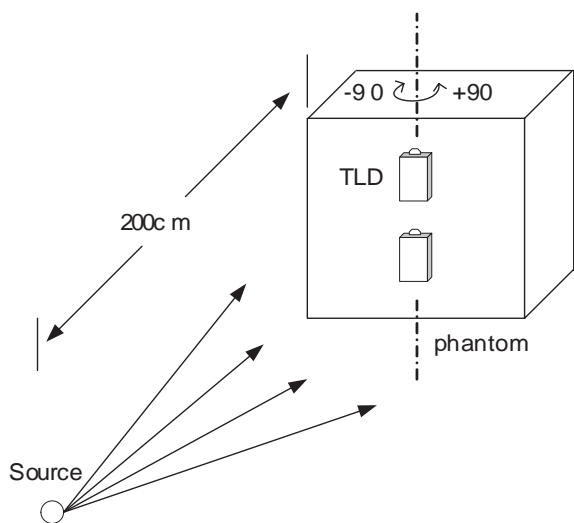


Fig. 9. The angular dependence experiments.

deep dose equivalent. For low-energy photons (ANSI M60, 35.2 keV) within the incidence angle of 60°, the dosimeter generally show the response within the maximum error of 12% compared to ARF. For higher energy photons (<sup>137</sup>Cs, 662 keV), the measurement within the incidence angle of 60° shows the maximum error of about 4%. It is expected that the dosimeter is perfectly angle independent in terms of the deep dose equivalent.

7. Conclusion

The TL dosimeter badge system based on newly developed LiF:Mg,Cu,Na,Si TL detectors was developed for personal radiation monitoring. It turned out that the badge

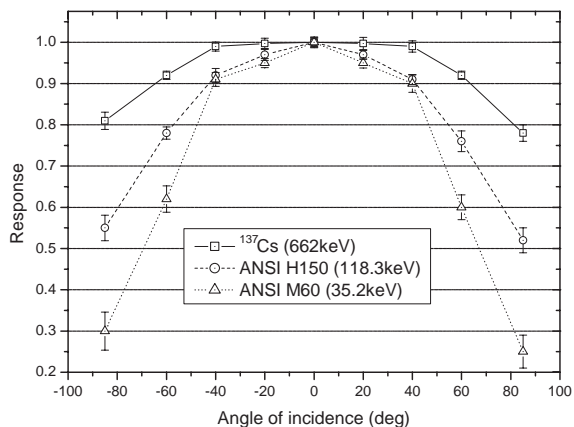


Fig. 10. Angular dependence of deep dose response of LiF:Mg,Cu,Na,Si TL dosimeter, normalized to response at normal incidence (0°), for three X-ray beams with an effective energy of 35.2, 118.3 and 662 keV from <sup>137</sup>Cs.

system of a TL dosimeter with LiF:Mg,Cu,Na,Si TL detector is suitable to estimate personal dose equivalent,  $H_p(d)$ , through the irradiation experiments for the dosimeter. With photon energy response results, the proposed TL dosimeter badge design meets the ±30% design limits required by the ISO standard and it shows a good characteristic for being applied for a personal radiation monitoring. The dosimeter also shows that it is able to discriminate the incident radiation type between photon and beta particle using certain ratios of the four TL detectors. Through the angular dependence test, the dosimeter was verified for its characteristic of angular dependence in terms of the deep dose equivalent. The TL dosimeter developed in this study is, therefore, feasible to be utilized in common TLD market. Although the feasibility of the LiF:Mg,Cu,Na,Si TL dosimeter was

Table 6  
Angular dependence of dosimeter in consideration of angular response factor

Beam code and angle of incidence	Angular response factor (ARF) in Table 4	Angular response of dosimeter				
		Clockwise (-)		Counterclockwise (+)		
		Response	Error (%)*	Response	Error (%)*	
ANSI M60	$\alpha = 40^\circ$	0.89	0.91	+2.2	0.90	+1.1
	$\alpha = 60^\circ$	0.68	0.62	-8.8	0.60	-11.8
ANSI H150	$\alpha = 40^\circ$	0.94	0.92	-2.1	0.91	-3.2
	$\alpha = 60^\circ$	0.82	0.78	-4.9	0.76	-7.3
<sup>137</sup> Cs	$\alpha = 40^\circ$	0.99	0.99	0.0	0.99	0.0
	$\alpha = 60^\circ$	0.96	0.92	-4.2	0.92	-4.2

\* Note that Error (%) =  $\{(Response - ARF)/ARF\} \times 100$ .

demonstrated in photon fields, more intensive work for the dosimetric properties of the dosimeter for mixed radiation field is need. In addition, more comprehensive researches including the performance test related to dose assessment algorithm is required to meet the ultimate object of a personal TL dosimeter in the future.

## References

- American National Standard Institute, 1999. American National Standard for Dosimetry—Personal dosimetry performance criteria for testing. ANSI N13.11.
- Bos, A.J.J., 2001. High sensitivity thermoluminescence dosimetry. *Nucl. Instr. Methods Phys. Res. B* 184, 3–28.
- Budzanowski, M., Kim, J.L., Nam, Y.M., Chang, S.Y., Bilski, P., Olko, P., 2001. Dosimetric properties of sintered LiF:Mg,Cu,Na,Si TL detectors. *Radiat. Meas.* 33, 537–540.
- Daniel, F., Boyd, C.A., Sanders, D.F., 1953. *Science* 117, 343.
- Doh, S.H., Chu, M.C., Chung, W.H., Kim, H.J., Kim, D.S., Kang, Y.H., 1989. Preparation of LiF (Mg,Cu,Na,Si) phosphor and its thermoluminescent characteristics. *Korean Appl. Phys.* 2, 425–431.
- ISO, 1984. Personal and Environmental Thermoluminescence Dosimeters, ISO Standards DP 8034.
- Kim, H.J., Chung, W.H., Doh, S.H., Chu, M.C., Kim, D.S., Kang, Y.H., 1989. Thermoluminescence dosimetric properties of LiF(Mg,Cu,Na,Si). *J. Korean Phys. Soc.* 22, 415–420.
- Kim, J.L., Kim, B.H., Chang, S.Y., Lee, J.K., 1997. Establishment of ANSI 13.11 X-ray radiation fields for personal dosimetry performance test by computational and experiment. *Environ. Health Perspect.* 105 (6), 1417–1422.
- Lee, J.I., Kim, J.L., Yang, J.S., Kim, B.Y., Nam, Y.M., 2002. Development of highly sensitive LiF:Mg,Cu,Na,Si TL detector. The First Asian and Oceanic Congress for Radiation Protection (AOCR-1).
- Moscovitch, M., 1993. Dose algorithms for personal thermoluminescence dosimetry. *Radiat. Prot. Dosimetry* 47 (1/4), 373–380.
- Nakajima, T., Maruyama, Y., Matsuzawa, T., Koyano, A., 1978. A development of a new highly sensitive LiF thermoluminescence dosimeter and its application. *Nucl. Instrum. Methods* 157, 155–162.
- Nam, Y.M., Kim, J.L., Chang, S.Y., Kim, G.D., 1998. The study of glow curves for LiF:Mg,Cu,Na,Si phosphor with different dopant concentrations. *Ungyong Mulli* 11, 578–583.
- Nam, Y.M., Kim, J.L., Chang, S.Y., 1999. Dependence of glow curve structure on the concentration of dopants in LiF:Mg,Cu,Na,Si phosphor. *Radiat. Prot. Dosimetry* 84, 231–234.
- Nam, Y.M., Kim, J.L., Chang, S.Y., Doh, S.H., 2000. Fabrication of LiF:Mg,Cu,Na,Si Pellets by Sintering Process. *Saemulli* 40 (3), 189–193.
- Nam, Y.M., Kim, J.L., Chang, S.Y., 2001. Dosimetric properties of LiF:Mg,Cu,Na,Si TL pellets. *J. Korean Assoc. Radiat. Prot.* 26 (1), 1–6.
- ORNL, 1994. SABRINA Three-Dimensional Geometry Visualization Code System Version 3.54 Manual, PSR-242.
- Radiation Safety Information Computational Center (RSICC), 2000. MCNP: A general Monte Carlo n-particle transport code version 4C.
- Vij, D.R., 1993. Thermoluminescent Material. Prentice-Hall, Englewood Cliffs, NJ.
- Will, W., 1991. Energy independent measurement of photon individual dose equivalents with LiF detectors behind combined filters. *Radiat. Prot. Dosimetry* 36 (1), 55–58.